A Flexible, Highly Sensitive, and Selective Chemiresistive Gas Sensor Obtained by In Situ Photopolymerization of an Acrylic Resin in the Presence of MWCNTs

Macromolecular Materials and Engineering
www.mme-journal.de

A Flexible, Highly Sensitive, and Selective Chemiresistive Gas Sensor Obtained by In Situ Photopolymerization of an Acrylic Resin in the Presence of MWCNTs

*Lorenzo Vigna, Andrea Fasoli, Matteo Cocuzza, Fabrizio C. Pirri, Luisa D. Bozano, and Marco Sangermano**

A new flexible polymeric gas sensor is developed by photocrosslinking poly(ethylene glycol) diacrylate resin (PEGDA) containing multi-walled carbon nanotubes (MWCNTs) as conductive filler. The cured material shows a percolative threshold conductivity which changes when in contact with various gas analytes with different chemical and physical properties. The different behavior of the sensors toward the different gases is explained either on the basis of chemical affinity toward the polymeric matrix or due to the interactions that can occur between the analyte and the surface of the nanotubes in the case of the aromatic gas.

1. Introduction

The development of miniature and portable gas sensors able to detect gas analytes in real time with good sensing performances will significantly change our daily life. In the scientific literature there is a large interest for these sensors where the improvement of sensitivity and selectivity is required.[1–4] Metal oxide semiconductors,[5–7] conducting polymers,[8–10] and composites[11–13] are among the most commonly utilized materials employed in building these devices. Even if the sensing mechanism is different for the three cited materials, the working principle behind them is always the same. They are called chemiresistor sensors because the transduction mechanism implicates the adsorption of the gas on the sensor surface with a consequent clear electric resistance variation, which is usually seen as a change in the output current.[14,15]

Among chemiresistive gas sensors polymer composites are the best choice when flexibility is required. Furthermore, they have several unique attractive features such as versatility, lightweight, low energy consumption and operational temperature, low cost, and the potential to be adapted for many different applications.[16]

Most polymers are insulating materials, but they will acquire certain conductivity through dispersing conductive fillers. When the amount of the conductive filler allows the formation of conductive paths throughout the matrix, the resistivity decreases by many orders of magnitude.[17] The phenomenon is known as percolation and can be well-explained by percolation theory.[18,19]

Some authors have already proposed the use of carbon nanotubes (CNTs), as conductive filler, to be dispersed within a polymeric matrix and used the composites as vapor sensors.[20–24] The changes in electrical resistivity of these composites are measured and are attributed to the swelling of the polymer matrix and/or conductive modification due to the solvent absorption. Upon the exposure to a gas, the polymeric composites reversibly swell to varying degrees according to the polymer–gas interactions. The swelling induces a change in conductivity that can easily be monitored. This happens because the swelling expands the inter-particulates distance and partially destroys the conductive networks. As a result, a drastic rise in resistivity of the materials is perceived.

This swelling-sensing method has been exploited by different authors where the mechanism involved is generally described by the so-called percolation theory and swelling.[25–27] Yoon et al.[28] showed that different gas concentrations diffusing into the polymer affect the distance between carbon nanotubes through polymer swelling. Dong et al. demonstrated that polymer composites filled with carbon black as conductive filler, exhibit remarkable increase in resistivity as soon as the composites are exposed to certain organic vapors.[29–32]

The swelling behavior is a reversible process because the vapor molecules are not chemically bound and so they desorb, allowing the fillers to regenerate the conductive paths and the sensor can be re-used. A relevant parameter is the solubility of

L. Vigna, Prof. M. Cocuzza, Prof. F. C. Pirri, Prof. M. Sangermano
Department of Applied Science and Technology (DISAT)
Politecnico di Torino
C.so Duca degli Abruzzi 24, 10129 Torino, Italy
E-mail: marco.sangermano@polito.it
Prof. M. Cocuzza
CNR-IMEM
Parco Area delle Scienze, 37a, 43124 Parma, Italy
Dr. A. Fasoli, Dr. L. D. Bozano
IBM Almaden Research Center
650 Harry Road, 95120 San Jose, CA, USA
Prof. F. C. Pirri
Istituto Italiano di Tecnologia
Center for Sustainable Future Technologies
Corso Trento, 21, 10129 Torino, Italy
The ORCID identification number(s) for the author(s) of this article can be found under https://doi.org/10.1002/mame.201800453.

DOI: 10.1002/mame.201800453

the polymer in the solvent and the affinity between the matrix and the variety of analytes through different functional groups because they can highly influence the level of swelling and a certain degree of selectivity.

Taking into account this background, in this work we have developed new polymer-composite gas sensors by dispersing multi-walled carbon nanotubes (MWCNTs) into an UV-curable acrylic resin. This method allows to obtain flexible sensors even on relatively thick films (hundreds of microns) either deposited on substrates or self-standing. In particular, the use of photopolymerization is attractive since the conductive filler is previously dispersed within the polymeric precursor and the composite is quickly formed by a short UV-irradiation occurring at room temperature, so that the sensor could be deposited also on thermal sensitive substrates.

The MWCNTs were dispersed into poly (ethylene glycol) diacrylate (PEGDA), the UV-curing conditions were evaluated, and conductivity measured on cross-linked films to evaluate the percolation threshold. Finally, the sensitivity and selectivity of these materials toward different gas analytes were evaluated by means of a detection chamber connected to a gas delivery system.

2. Experimental Section

2.1. Materials

Acrylic resin, poly(ethylene glycol) diacrylate (average molecular weight M_n 575, **PEGDA**), and poly(ethylene glycol) methyl ether methacrylate (average molecular weight M_n 500, **PEGMEMA)** were purchased from Sigma-Aldrich. The liquid radical photoinitiator 2-hydroxy-2-methyl-1-phenyl-propan-1-one (Darocur 1173, D-1173), was formally supplied by BASF. The carbonaceous filler used was **MWCNTs** NC3100 kindly provided by Nanocyl. All the chemicals were used as received without further purification.

2.2. Nanocomposite Films Preparation

The typical UV-cured sample was prepared as follows: the MWCNTs (in the range between 0.1–1 wt% with respect to the resin content) were added to the PEGMEMA and dispersed using a Sonifier (Branson 250) for 30 min at 10% of intensity (2–3 W). Then, the radical photoinitiator (3 wt% with respect to the resin) and the PEGDA resin were added and homogenized using a high-shear homogenization (Ultraturrax IKA T10) for 5 min at 30 000 rpm. The ratio between the PEGDA and the PEGMEMA was 1:1.5. The PEGMEMA was added principally to reduce the viscosity of the photocurable nanocomposite. Subsequently, the liquid formulation was poured in a PDMS mold and then cured for 5 min under nitrogen atmosphere by using a UV-light medium pressure mercury lamp (Dymax ECE) with a light intensity on the surface of the sample of about 82 mW cm^{-2} (measured with EIT photometer). After irradiation and unmolding, tack-free self-standing films of about 25 × 25 mm^2 with a thickness of about 500 µm were obtained.

2.3. Electrodes Deposition

In order to perform the electrical characterization on the cross-linked materials, interdigitated gold electrodes (IDEs) were deposited on top of the films by means of a custom-made evaporator that exploited a stainless steel shadow mask of the desired pattern. A 3 nm thin layer of chromium was evaporated in order to promote the adhesion of the following 100 nm of gold that ensures the contact. Each electrode was composed of six fingers interdigitated one with each other. The length and width of a single finger were 12 and 1 mm, respectively. The distance between the two pads was 15 mm.

2.4. Characterization

2.4.1. FTIR

Fourier-transform infrared spectroscopy (FTIR) analyses were performed in transmission mode using an Infrared spectrophotometer (Thermo Electron Corporation). The solutions were analyzed after being applied onto a silicon wafer and UV-cured. A film of 25 µm was coated on the silicon wafer and the analysis was carried out with a resolution of 4 cm^{-1} and samples were scanned 32 times in the wavenumber range between 650 and 4000 cm^{-1}. A background measurement was performed before each of the samples were subjected to FTIR analysis. The analyses were run collecting spectra during 1 min of irradiation, in order to evaluate the final conversion. The acrylate double bonds conversion during irradiation was calculated following the peak area of C=C group at 1640 cm^{-1} and normalized with the peak area of C=O group at 1730 cm^{-1}.

2.4.2. Sensing Setup

The sensing characterizations were carried out by using a custom-made sensing setup in order to produce and deliver selected concentrations of solvent vapors to the samples. In the system, a stream of oil-free dry air (relative humidity, RH < 2%) was exploited as carrier and diluting gas. The main stream was divided into two fluxes regulated by the presence of two mass flow controllers (MFC) supplied by MKS. The carrier gas flows through a thermostatic chamber composed of a bubbler evaporation system placed inside a Dewar flask and properly filled with the volatile organic compound (VOC) to be tested. Past the bubbler, the two flows were recombined, mixed, and directed to a detection chamber made of a stainless steel assembly with a 39 mm inner diameter. The operational temperature for the sensing measurements herein reported was 19 °C. A constant flow of 100 sccm was set to impinge the samples. All the experiments carried out in this work exploited five different analytes: acetone, ethanol, isopropanol, toluene, and water. The concentration in part per million (ppm) of the volatile vapor was calculated using the following equation:

$$C(\text{ppm}) = \left(\frac{P^*}{P} \times \frac{f}{f+F}\right) \times 10^6 \quad (1)$$

where P is the input air pressure (atmospheric pressure in this case), P^* is the saturated partial pressure of the analyte, f and F are the mass flow rate of MFC of the pure dry air and MFC of the carrier, respectively. P^* is evaluated by Antoine's equation as a function of the temperature and Antoine's component-specific constants A, B, and C.[33,34]

$$P^* = 10^{\left(A - \frac{B}{C+T}\right)} \quad (2)$$

2.4.3. Sensing Analysis

The electrical resistance was investigated by using two-probes measurements, exploiting a Keithley model 6430 SourceMeter and an impedance analyzer 4294A supplied by Agilent. Two different sensing analyses were performed: DC and AC tests. In the DC analysis, 100 mV voltage was applied between the electrodes and the current was acquired as a function of the time. For each test, dry air was introduced for 100 s in order to get the current baseline. Successively, the sensor was exposed to the analyte at the desired concentration for 600 s, followed by further 600 s that was set as recovery time. The other measurements were carried out in AC ranging from 40 Hz up to 110 MHz.

AC measurements offer greater insights than DC into the charge transport properties of the sensing films, as they allow to extract capacitive and inductive components, in addition to the resistive ones, and to potentially discriminate between contributions arising by distinct transport mechanisms or from different elements of the device under test. The nanocomposite film was exposed to a flux of dry air overnight for more than 12 h before starting the measurements. The first snapshot was taken as reference in dry air. The second one was captured after having exposed the film for 600 s in an environment with different concentrations of the volatile organic compound (VOC) analyte (ethanol or acetone). In order to evaluate the recovery of the film, dry air was flushed for further 600 s and the test run again. The data were then processed with a Matlab script and the output results were interpreted from the Nyquist plots.

The typical response of the sensor to a particular gas (S) is calculated as the ratio between the steady-state resistance variation ΔR and the baseline resistance of the device:

$$S = \frac{\Delta R}{R_{\text{Baseline}}} \quad (3)$$

In this work, the formula used is reported below:

$$S^* = \frac{I_{\text{Air}}}{I_{\text{Gas}}} = \frac{R_{\text{Gas}}}{R_{\text{Baseline}}} = S + 1 \quad (4)$$

3. Results and Discussion

The aim of this study was the preparation of a flexible polymer-composite gas sensor showing a good sensitivity and a certain degree of selectivity toward different gases and responding to the presence of the gas toward an enhancement of resistivity as a consequence of a swelling behavior when in contact with a certain gas. For this purpose, UV-cured PEGDA films were prepared in the presence of MWCNTs as conductive filler.

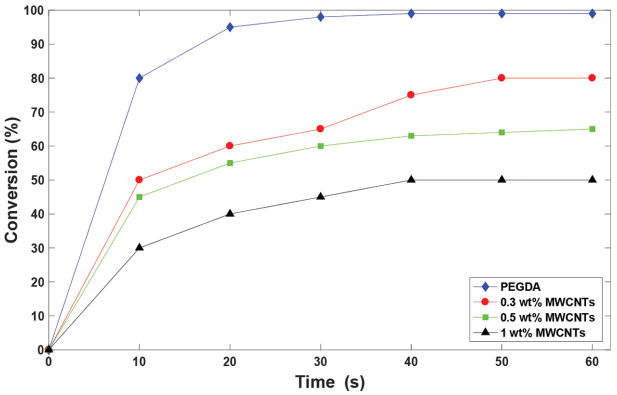

Figure 1. Conversion curves as a function of MWCNTs dispersed into PEGDA. Photoinitiator always at 1 wt%, light intensity during irradiation 82 mW cm^{-2}. Film thickness 25 µm.

As a first step we have evaluated the reactivity of the photocurable formulations in the presence of MWCNTs. It was evidenced, by FTIR analysis, that an increase of the MWCNTs content in the photocurable formulations induced an important decrease on both acrylic double bond conversion and rate of photopolymerization (**Figure 1**).

While the pristine PEGDA is characterized by a high reactivity achieving 100% of acrylic double bond conversion after few seconds of irradiation, the same resin showed a decrease of the final double bond conversion to a value of 50% in the presence of 1 wt% of MWCNTs filler and 1 wt% of radical photoinitiator.

This is a very well-known phenomenon mainly due to the strong absorption of light by the MWCNTs, which strongly compete with the light adsorption of the photoinitiator.[33] We overcame this problem on the basis of our previous experience[34,35] by adjusting parameters such as the radical photoinitiator content. In **Figure 2** the conversion curves as a function

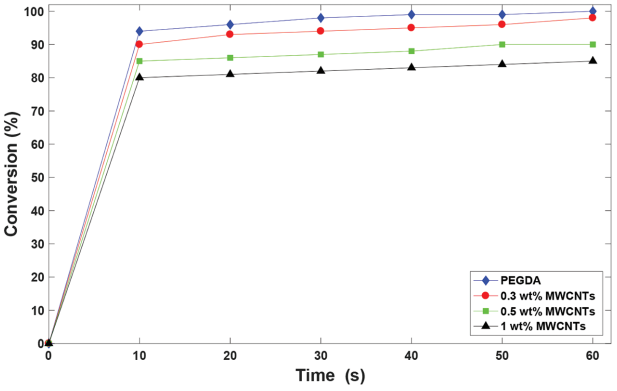

Figure 2. Conversion curves as a function of MWCNTs dispersed into PEGDA. Photoinitiator always at 3 wt%, light intensity during irradiation 82 mW cm^{-2}. Film thickness 25 µm.

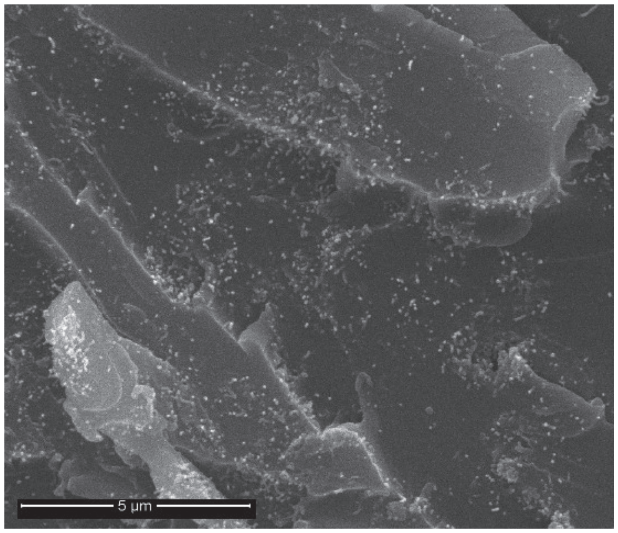

Figure 3. FESEM image obtained from the fracture surface of the PEGDA cross-linked film containing 0.3 wt% of CNTs.

of irradiation time are reported for the same PEGDA-based formulations containing MWCNTs, increasing the amount of radical photoinitiator from 1 wt% up to 3 wt%.

It is evident that by increasing the photoinitiator content up to 3 wt% it is possible to reach, for all the formulations, an almost complete acrylic double bond conversion. Therefore, cross-linked films were prepared in the presence of 3 wt% of radical photoinitiator.

Electrical characterizations were performed on cured films with a thickness of about 600 µm. An enhancement in conductivity for the cross-linked films obtained in the presence of MWCNTs was observed. This can be related to the formation of a percolating path among CNTs that allows the electrical conduction.[36–39]

In **Figure 3**, the FESEM morphological analysis has been reported for the surface fracture of the PEGDA cross-linked film containing 0.3 wt% of CNTs. A homogeneous dispersion of the conductive fillers is evident, in accordance with the percolation values.

The resistance for the cross-linked PEGDA film containing 0.3 wt% of MWCNTs was evaluated to be 2.13 kΩ. Further increase of conductive filler did not significantly enhance the conductivity, while adversely affecting the viscosity. For this reason, the cross-linked films containing 0.3 wt% of MWCNTs were selected for gas sensors evaluation. This composite film is at the percolative concentration and allows reaching a complete cross-linked film upon irradiation.

The selected composite film was exposed for 600 s to an environment with different concentrations of ethanol and acetone. During the film exposure to gas, measurements were carried out in AC over the whole spectrum ranging from 40 Hz up to 110 MHz, and Nyquist plots were recorded. In **Figure 4** the Nyquist plots for the PEGDA film containing 0.3 wt% of MWCNTs are reported, as an example, when the film is exposed to acetone atmosphere at a concentration of 11 500 ppm.

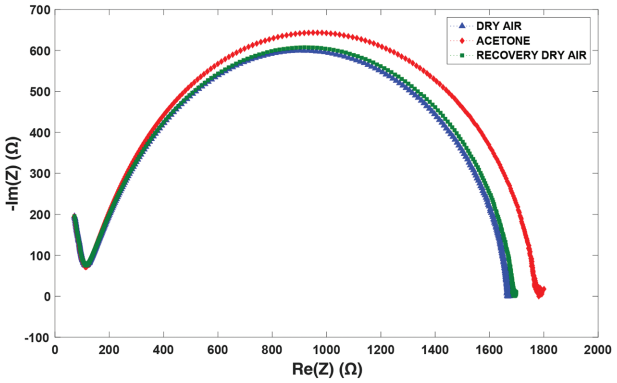

Figure 4. Static analysis of the MWCNTs-based sensor with relative Nyquist plots.

By modeling the composite film as a parallel between a resistance R and a capacitance C, the main arc can be fitted by the relationship:

$$Z = \frac{R}{1 + i\omega RC} \tag{5}$$

where Z is the film impedance and ω the angular frequency.

This allows to extract the resistance of the film and to follow its change upon exposure to a given analyte (Figure 4). In addition, from the graph it is possible to observe the beginning of a second arc. This is sign of a separate contribution, possibly arising from the injection of charges at the interface between the filler and the electrodes.

The resonance frequency, calculated as the frequency of the maximum of the curve, does not show a significant shift. Similar plots were registered for the films exposed to either acetone or ethanol at different concentrations. All the values extracted from the single experiments are collected in **Table 1**.

As expected, the resistance increases when the film gets in contact with the target analyte and it recovers to the original value almost every time when it is dried. A similar behavior can be found for the capacitance.

The recoverability of the composites resistivity is achieved once the specimen was exposed to dry air after removing the analyte vapors. It is found that the composites resistance quickly recovers to the initial value (Figure 4). Such fast recovery is attributable to the mobility of the fillers in the gas-swollen composite, leading to the re-aggregation of MWCNTs and reconstruction of the damaged conductive networks occurred during swelling.

The AC analysis was performed and compared with the DC measurements carried out on the sample in terms of electrical response, following the protocol reported in the Experimental Section.

In order to evaluate the selectivity of the proposed polymeric sensor, five analytes with different chemical and physical properties were investigated: one ketone (acetone), two alcohols (ethanol and isopropanol), an aromatic compound (toluene), and the water vapor. Different gas flows were used because the analytes have different vapor pressures (water < toluene < isopropanol < ethanol < acetone). For this reason, the flows

Table 1. Resistance values for the cross-linked PEGDA film containing 0.3 wt% of MWCNTs in contact with different concentrations of acetone and ethanol.

Matrix	Analyte	Concentration [ppm]	R_0 [kΩ]			C_0 [pF]			Sensitivity [S*]
			Dry air	Analyte	Recovery	Dry air	Analyte	Recovery	
PEGDA 575 + MWCNT	Acetone	11 600	1.559	1.559	1.547	581.9	594.9	580.3	1.02
	Acetone	23 200	1.540	1.610	1.568	579.3	611.0	582.3	1.05
	Acetone	46 400	1.562	1.671	1.582	581.0	637.4	583.4	1.10
	Ethanol	2700	1.433	1.437	1.432	546.1	551.5	546.6	1.01
	Ethanol	5400	1.469	1.479	1.476	548.9	558.3	558.1	1.02
	Ethanol	11 300	1.460	1.491	1.463	547.7	568.9	548.1	1.04
	Ethanol	23 200	1.451	1.560	1.488	547.0	592.1	546.2	1.08

were carefully chosen to achieve similar levels of concentration between different analytes.

In **Figure 5**, the sensing curves of all the five various analytes related to concentrations ranging from 10 000 up to 23 000 ppm are reported. The initial current for each experiment, in dry air, ranges from 58.2 to 61.1 μA, sign that prior exposure to each analyte the MWCNT's network is in similar configurations.

By observing the curves reported in Figure 5, it is possible to state that the drop in current and its recovery are faster for toluene and isopropanol. On the contrary, acetone, water, and ethanol curves present drops with a reduced slope and the recovery time is longer. In the case of ethanol, the recovery is incomplete, within the timescale shown in the figure.

A study on the stability of the film was carried out, where the sample was exposed to repeated cycles of toluene exposure, at the same concentration, over the course of 3 h (Figure 5e). Although full recovery is not always achieved, the four cycles still show the same relative change in current. The last cycle shows that the recovery is eventually reached over a longer timescale. This is an encouraging result because it shows that the MWCNT's matrix can be reconstituted over multiple sensing cycles so that the sensor retains its sensing properties.

The results can be collected in a graph where sensitivity as a function of analyte concentration is reported (**Figure 6**).

It appears that the electrical response increases in different ways as the analytes concentration increases. The affinity toward acetone is the smallest. In fact, the ketone has very little polarity, while the PEGDA polymer is highly polar. Ethanol and propanol, instead, show a similar response. This is reasonable because they both belong to the same class and have very similar polarity. The sensitivity along with water is much higher with respect to the acetone. This can be explained by the strong hydrogen-bonding interactions among water and PEGDA matrix, which could allow to reach a higher swelling degree and therefore a higher increase of resistivity when the conductive polymeric film comes in contact with the analyte. However, quite surprisingly, the best response is toward toluene, that has no polar groups and it is strongly non-polar. This fact might be explained with interactions that could occur between the analyte and the surface of the nanotubes dispersed into the polymeric matrix. A possible π–π interaction among the aromatic ring of the analyte and the conductive filler could be responsible for the disruption of the percolation network, with an important enhancement of the resistivity of the film in the presence of the aromatic compound.

4. Conclusions

The aim of this work was the development of improved gas sensors characterized by sensitivity, selectivity, and stability. For this reason, PEGDA UV-cured composite films were prepared by dispersing MWCNTs as conductive filler. The best photo-curing conditions were evaluated and the films obtained in the presence of 0.3 wt% of MWCNTs showed a percolative threshold conductivity. The films can be self-standing or coated on different substrates and are stable to the presence of gas vapors because they are cross-linked films. Their resistivity enhancement, when in contact with the gas analyte, was measured either in AC and DC mode performed in a chamber connected to a gas delivery system.

Analyzing the MWCNT-based sensors, the results obtained in DC are consistent with the AC measurements. This new material looks very promising because the sensors show good sensitivity as well as selectivity toward various analytes. Five analytes with different chemical and physical properties were investigated: one ketone (acetone), two alcohols (ethanol and isopropanol), an aromatic compound (toluene), and water vapor. The affinity toward acetone is the smallest, while ethanol and propanol show a similar response. The sensitivity along with water is much higher with respect to the acetone, while the best response is toward toluene. The different behavior of the sensors toward the different gases was explained either on the basis of chemical affinity toward the polymeric matrix or due to the interactions that could occur between the analyte and the surface of the nanotubes in the case of the aromatic gas. Further improvements could be reached by a simple modification of the photocurable mixture, modifying the chemistry of the resin and therefore the affinity toward polar or non-polar gases.

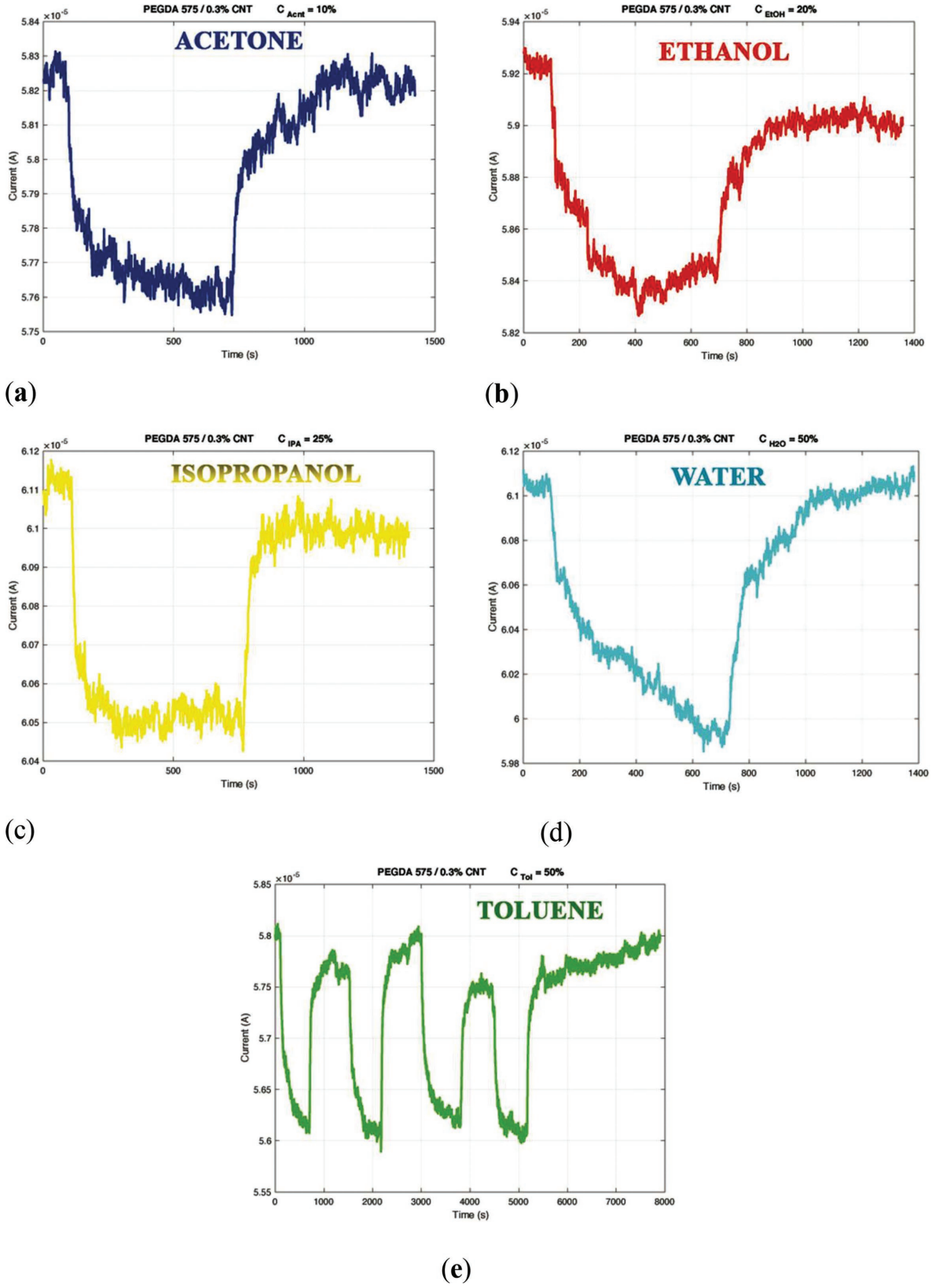

Figure 5. Sensing response of MWCNTs-based sensor toward similar concentrations of a) acetone, b) ethanol, c) isopropanol, d) water, and e) toluene.

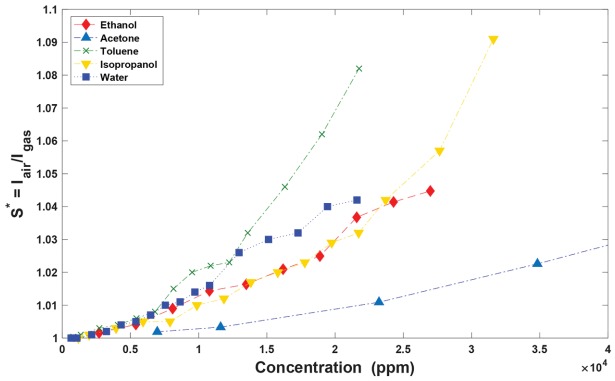

Figure 6. Sensitivity as a function of gas content for the different tested gas analytes.

Conflict of Interest

The authors declare no conflict of interest.

Keywords

carbon nanotubes, chemiresistors, conductive polymer nanocomposites, gas sensors, UV-curing, VOC detection

Received: July 27, 2018
Revised: September 17, 2018
Published online: October 17, 2018

[1] Y. Wang, J. T. W. Yeow, *J. Sens.* **2009**, *2009*, 1.
[2] S. M. Cho, Y. J. Kim, Y. S. Kim, Y. Yang, S.-C. Ha, *Proc. IEEE Sens.* **2004**, *2*, 701.
[3] T. K. Gupta, K. Shanmugam, *Carbon Nanotube-Reinf. Polym.* **2018**, *1*, 61.
[4] A. Kausar, I. Rafique, B. Muhammad, *Polym.-Plast. Technol. Eng.* **2016**, *55*, 1167.
[5] G. Korotcenkov, *Mater. Sci. Eng. B*, **2007**, *139*, 1.
[6] I. Simon, N. Bârsan, M. Bauer, U. Weimar, *Sens. Actuators, B* **2001**, *73*, 1.
[7] M. A. Carpenter, S. Mathur, A. Kolmakov, *Metal Oxide Nanomaterials for Chemical Sensors*, Springer, New York **2013**. https://doi.org/10.1007/978-1-4614-5395-6
[8] N. Razza, B. Blanchet, A. Lamberti, F. C. Pirri, J.-M. Tulliani, L. D. Bozano, M. Sangermano, *Macromol. Mater. Eng.* **2017**, *302*, 1700161.
[9] A. C. Partridge, M. L. Jansen, W. M. Arnold, *Mater. Sci. Eng. C* **2000**, *12*, 37.
[10] H. Bai, G. Shi, *Sensors* **2007**, *7*, 267.
[11] B. Zhang, R. W. Fu, M. Q. Zhang, X. M. Dong, P. L. Lan, J. S. Qiu, *Sens. Actuators, B* **2005**, *109*, 323.
[12] S. Badhulika, N. Myung, A. Mulchandani, *Talanta* **2014**, *123*, 109.
[13] J. Lee, D. Cho, Y. Jeong, *Solid-State Electron.* **2013**, *87*, 80.
[14] K. Arshak, E. Moore, G. M. Lyons, J. Harris, S. Clifford, *Sens. Rev.* **2004**, *24*, 181.
[15] K. J. Albert, N. S. Lewis, C. L. Schauer, G. A. Sotzing, S. E. Stitzel, T. P. Vaid, D. R. Walt, *Chem. Rev.* **2000**, *100*, 2595.
[16] H. T. Nagle, R. Gutierrez-Osuna, S. S. Schiffman, *IEEE Spectrum* **1998**, *35*, 22.
[17] J. N. Coleman, S. Curran, A. B. Dalton, A. P. Davey, Mc B. Carthy, W. Blau, R. C. Barklie, *Synth. Met.* **1999**, *102*, 1174.
[18] B. C. Muñoz, G. Steinthal, S. Sunshine, *Sens. Rev.* **1999**, *19*(4), 300.
[19] M. C. Lonergan, E. J. Severin, B. J. Doleman, S. A. Beaber, R. H. Grubbs, N. S. Lewis, *Chem. Mater.* **1996**, *8*, 2298.
[20] C. Li, E. T. Thostenson, T.-W. Chou, *Compos. Sci. Technol.* **2008**, *68*, 1227.
[21] C. Wei, L. Dai, A. Roy, T. B. Tolle, *J. Am. Chem. Soc.* **2006**, *128*, 1412.
[22] J. Chen, N. Tsubokawa, *Polym. J.* **2000**, *32*, 729.
[23] M. Castro, J. Lu, S. Bruzaud, B. Kumar, J.-F. Feller, *Carbon* **2009**, *47*, 1930.
[24] Q. Fan, Z. Qin, T. Villmow, J. Pionteck, P. Pötschke, Y. Wu, B. Voit, M. Zhu, *Sens. Actuators, B* **2011**, *156*, 63.
[25] B. Philip, J. K. Abraham, A. Chandrasekhar, V. K. Varadan, *Smart Mater. Struct.* **2003**, *12*, 935.
[26] J. A. Covington, J. W. Gardner, D. Briand, N. F. de Rooij, *Sens. Actuators, B* **2001**, *77*, 155.
[27] B. Zhang, R. W. Fu, M. Q. Zhang, X. M. Dong, P. L. Lan, J. S. Qiu, *Sens. Actuators, B* **2005**, *109*, 323.
[28] H. Yoon, J. Xie, J. K. Abraham, V. K. Varadan, P. B. Ruffin, *Smart Mater. Struct.* **2006**, *15*, S14.
[29] X. M. Dong, R. W. Fu, M. Q. Zhang, B. Zhang, J. R. Li, M. Z. Rong, *Carbon* **2003**, *41*, 371.
[30] X. M. Dong, R. W. Fu, M. Q. Zhang, B. Zhang, M. Z. Rong, *Carbon* **2004**, *42*, 2551.
[31] J. F. Gao, H. Wang, X. W. Huang, M. J. Hu, H. G. Xue, R. K. Y. Li, *Compos. Sci. Technol.* **2018**, *161*, 135.
[32] J. F. Gao, H. Wang, X. W. Huang, M. J. Hu, H. G. Xue, R. K. Y. Li, *J. Mater. Chem. A* **2018**, *6*, 10036.
[33] J. A. Dean, A. L. Norbert,*Lange's Handbook of Chemistry*, 15th ed., McGraw-Hill, New York **1999**. https://doi.org/10.1002/jps.2600680645
[34] E. Araujo-Lopez, J. S. Lopez-Echeverry, S. Reif-Acherman, *Chem. Eng. Sci.* **2018**, *177*, 89.
[35] J. H. Sandoval, R. B. Wicker, *Rapid Prototyp. J.* **2006**, *12*, 292.
[36] G. Gonzalez, A. Chiappone, I. Roppolo, E. Fantino, V. Bertana, F. Perrucci, L. Scaltrito, F. Pirri, M. Sangermano, *Polymer* **2017**, *109*, 246.
[37] M. Sangermano, A. Vitale, N. Razza, A. Favetto, M. Paleari, P. Ariano, *Polymer* **2015**, *56*, 131.
[38] W. Bauhofer, J. Z. Kovacs, *Compos. Sci. Technol.* **2009**, *69*, 1486.
[39] P. H. da S. L. Coelho, M. S. Marchesin, A. R. Morales, J. R. Bartoli, *Mater. Res.* **2014**, *17*, 127.